

Effects of Shock-Tube Cleanliness on Slender-Body Hypersonic Instability and Transition Studies at High Enthalpy

N. J. Parziale*

Stevens Institute of Technology, Hoboken, NJ 07030, USA

J. S. Jewell†

Air Force Research Laboratory, WPAFB, OH 45433, USA

I. A. Leyva‡

Air Force Office of Scientific Research, Arlington AFB, VA 22203, USA

J. E. Shepherd§

California Institute of Technology, Pasadena, CA, 91125, USA

A series of slender-body hypervelocity boundary-layer instability and transition experiments were performed in the Caltech T5 Reflected-Shock Tunnel. During this campaign, it became clear that the condition of the T5 shock tube would significantly affect the consistency of the instability and transition measurements; a regimen of cleaning was iterated on until satisfactory repeatability was achieved. In this work, a description of the cleaning regimen is given. Additionally, boundary-layer instability measurements and a statistical analysis of the boundary-layer transition scatter are presented for experiments before and after cleaning regimen implementation.

I. Introduction

The prediction of high-speed boundary-layer transition (BLT) location is critical to hypersonic vehicle design; this is because increased skin friction and surface heating rate after transition result in increased weight of the thermal protection system (TPS). Studying this phenomena from a fundamental perspective is a necessary approach to advance the state of the art in BLT predictive science.

Typically, the approach is to perform experimental and computational studies in concert to elucidate the driving mechanisms of BLT. The free-stream disturbances in supersonic and hypersonic wind tunnels include acoustic waves, entropy inhomogeneity, and vortical perturbations, in addition to microscale and macroscale particulates.¹ These disturbances, in whatever form, can undermine BLT studies by altering the measured quantity such that confidence in the experimental measurements is compromised. Therefore, time should be invested in eliminating, or at the very least, minimizing and characterizing free-stream disturbance levels.

Hypersonic wind tunnels exist where there are low disturbance levels, such as those at Purdue²⁻⁴ and Texas A&M.⁵⁻⁷ Currently, the parameter space available to low-disturbance hypersonic wind tunnels does not permit the study of the interaction of boundary-layer instability and thermo-chemistry; this is because low-disturbance hypersonic tunnels have a low ordered kinetic energy, or total enthalpy, in the free-stream relative to relevant chemical or vibrational energy scales.

*Assistant Professor, Mechanical Engineering, Castle Point on Hudson, Hoboken, New Jersey, 07030. AIAA Member.

†Research Engineer (UTC Contractor), AFRL/RQHF, Wright-Patterson AFB, OH 45433. AIAA Member.

‡Program Officer, AFOSR/RTE, Arlington AFB, VA 22203. AIAA Associate Fellow.

§Professor, Graduate Aeronautical Laboratories, 1200 E. California Blvd., MC 105-50, USA. AIAA Senior Member.

To study the effects of thermo-chemistry on BLT in ground-test, the total enthalpy of the flow must be sufficiently high. One such ground-test facility to generate “high-enthalpy” flows is the reflected-shock tunnel. In the HEG reflected-shock tunnel, Laurence et al.^{8–10} report a schlieren-based technique for the investigation of disturbances in hypervelocity boundary layers. In those reports, high-resolution and time-resolved images of the second-mode instability of a hypervelocity boundary layer on a slender cone are presented. At Caltech in the T5 reflected-shock tunnel, Germain and Hornung,¹¹ Adam and Hornung,¹² Rasheed et al.,¹³ Jewell et al.,¹⁴ and Parziale et al.¹⁵ studied hypervelocity BLT on a slender cone; those researchers performed approximately 1000 experiments and made significant progress in developing visualization and direct measurement techniques. These diagnostic advances made possible the investigation of real-gas effects on BLT and hypervelocity BLT control by porous coatings. However, for the data in those reports, the researchers did not focus their efforts on performing experiments in the cleanest possible environment. Recently, Fedorov¹⁶ has examined receptivity to particulate-laden flows, modeling the particulates as spherical solids impacting the supersonic boundary layer, and making numerical estimates for particulate-driven transition onset for various sizes and densities. Fedorov found that both N factor and transition Reynolds number were strongly influenced by particle characteristics, including size and number density.

In this work, we describe a shock-tunnel operation procedure that was necessary to our more recent efforts^{17–23} where we achieved repeatable results while performing slender-body hypervelocity instability and transition ground-testing in T5. Through careful selection of conditions and cleaning of the shock tube, it is possible to systematically prescribe transition locations that are estimated to correspond to second-mode amplification factors e^N of $N \approx 8$ –12.^{22,23} These amplification values are high as compared to the more typical value of $N \approx 5$ –6 usually characterizing a “noisy” tunnel.² However, the high N factors are consistent with the expected difference in receptivity for the high-frequency second-mode instability as compared to the relatively low-frequency noise in the T5 free stream as measured by Parziale et al.²¹ This is supported by the recent analysis of Gronvall et al.²⁴ who found a transition onset value of $N \sim 8$ for the shock-tunnel experiments of Tanno et al.²⁵ Examples of data are presented from experiments before and after the cleaning regimen was instituted, and these results are compared.

II. Facility

All measurements are made in T5, the free-piston driven reflected-shock tunnel at the California Institute of Technology (Fig. 1). It is the fifth in a series of shock tunnels designed to simulate thermo-chemical effects on aerodynamics of vehicles flying at hypervelocity speeds through the atmosphere. More information regarding the capabilities of T5 can be found in the literature.²⁶

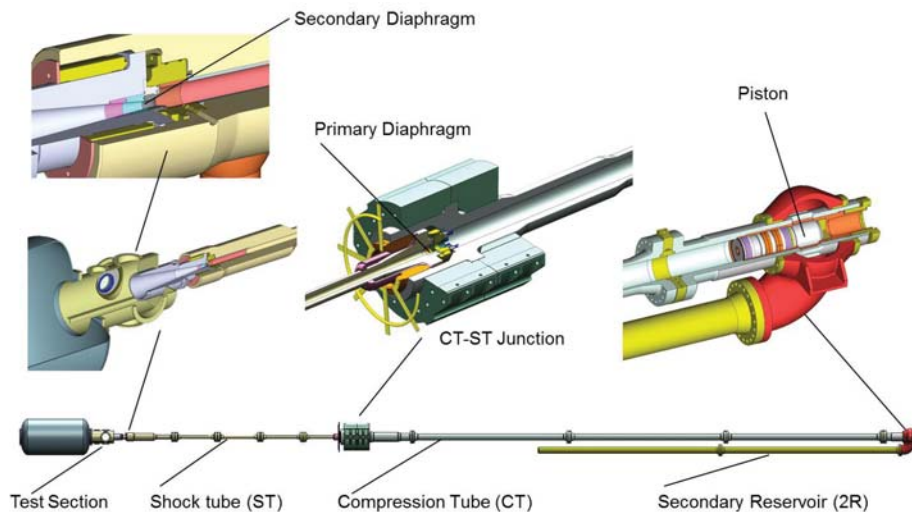


Figure 1. A schematic of T5 with a blown up view of each of the major sections.

An experiment is conducted as follows: a 120 kg aluminum piston is loaded into the compression tube/secondary reservoir junction. A secondary diaphragm (mylar, 127 μm thick) is inserted at the nozzle throat at the end

of the shock tube near the test section, and a primary diaphragm (stainless steel, 7 mm thick) is inserted at the compression tube/shock tube junction. The test section, shock tube, and compression tube are evacuated. The shock tube is filled with the test gas (in the present study, air and N_2 to 40-120 kPa), the compression tube is filled with a He/Ar mixture to ≈ 50 -100 kPa and the secondary reservoir is filled with air to ≈ 2 -10 MPa. The air in the secondary reservoir is released, driving the piston into the compression tube. This piston motion adiabatically compresses the driver gas of the shock tunnel to the rupture pressure of the primary diaphragm (≈ 30 -100 MPa). Following the primary diaphragm rupture, a shock wave propagates in the shock tube, is reflected off the end wall breaking the secondary diaphragm, and re-processes the test gas. The test gas is then at high temperature (≈ 4000 -9000 K) and pressure (≈ 20 -60 MPa) with negligible velocity, and is then expanded through a converging-diverging contoured nozzle to \approx Mach 5.5 in the test section.

Measured primary shock speed and reservoir pressure are used to compute the reservoir conditions for each shot. Thermo-chemical equilibrium calculations are performed using Cantera²⁷ with the Shock and Detonation Toolbox.²⁸ The appropriate thermodynamic data are found in the literature.^{29,30}

The steady expansion through the contoured nozzle from the reservoir to the free stream is modeled by the axisymmetric, reacting Navier Stokes equations as discussed by Candler³¹ and Wagnild.³² The boundary layer on the nozzle wall is assumed to be turbulent and modeled by one equation as in Spalart-Allmaras³³ with the Catris-Aupoix³⁴ compressibility correction. The grid is generated by the commercial tool, Gridgen. The mean flow over the cone is computed by the reacting, axisymmetric Navier Stokes equations with a structured-grid, and is part of the STABL software suite, as described by Johnson³⁵ and Johnson et al.³⁶ The boundary layer profiles and edge properties are extracted from the mean flow solutions during post-processing.

III. Shock Tube Fill Gas Quality and Cleaning Procedure

Throughout the testing campaign for this work, it became apparent that there was opportunity to increase the quality of the flow over the model from a technical standpoint. Improvement was achieved by using higher quality gas to fill the shock tube and cleaning the shock tube more thoroughly between experiments. Because consistent instability measurement results were obtained, the quality of the shock tube fill gas and shock tube cleaning procedure were fixed after shot 2760.

There is no apparent record of what grade of gas was used to fill the shock tube in previous work, but it was most likely “Industrial,” as it was when this test campaign started. According to specification sheets for “Industrial” air from Air Liquide (the gas bottle supplier), there is a large bound on the relative O_2 to N_2 balance ($\pm 2.5\%$ by partial pressure), and no clear quantification of total hydrocarbons (THC). According to the supplier, it is intended to be used for such purposes as powering pneumatic tools and inflating tires. Similarly loose specifications were found for “Industrial” grade N_2 and CO_2 . Throughout the development campaign, there was a switch to “Breathing Air,” then finally to the “ALPHAGAZ” line of gases. This last line of gases is intended to be used for research applications. The relative O_2 to N_2 balance is tighter ($\pm 0.5\%$ by partial pressure), and the THC are specified to be less than 0.05 ppm. Specifications for N_2 and CO_2 at this grade were found to be similarly acceptable.

At the beginning of this test campaign, standard shock tube cleaning practice in T5 was to roll four shop towels into a cylinder and drag them through the shock tube. It was hypothesized that reducing the particulates in the shock tube prior to the run could reduce the number of unexpected occurrences of particulate induced transition. The cleaning procedure between each experiment was changed to: 1) clean the shock-tube end with a Scotch-Brite pad, 2) clean the shock-tube end with acetone on a mop, 3) pass four shop towels rolled into a cylinder and drag them through the shock tube, the outer-most towel being misted with acetone, 4) repeat step 3 until the outermost towel does not become dirty after a pass through the shock tube.

The region at the end of the shock tube in a reflected-shock tunnel is an additional area of practical concern. In T5, this region (referring to left and top left of Fig. 1) is comprised of a copper insert and sleeve, shown in a larger view as Fig. 2. Taylor and Hornung³⁷ note that wall roughness in the reflected-shock region can increase the shock bifurcation asymptotic height. This behavior is undesirable because of the induced

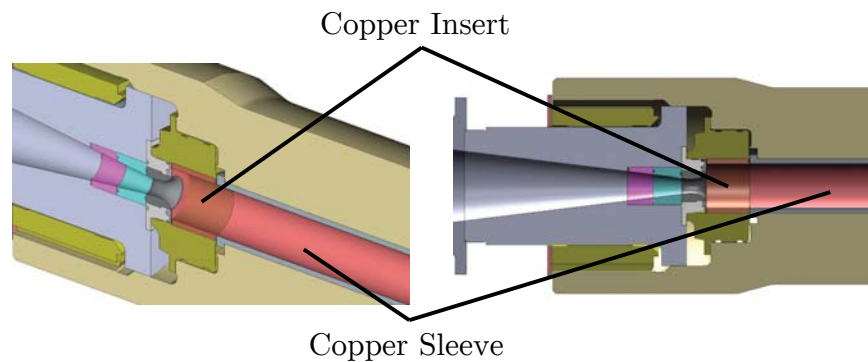


Figure 2. The copper sleeve and insert at the shock tube end. This is a larger view from Fig. 1.

non-uniformity of the reservoir gas³⁸ and decreased test time due to driver gas contamination of the reservoir gas.³⁹

After completing the cleaning regimen described previously, the copper insert and copper sleeve had a smooth finish. The roughness of the 90 mm diameter shock tube is estimated to be less than 25 μm . Throughout the test campaign the copper insert and sleeve were maintained in this condition to avoid the detrimental effects of shock bifurcation as much as possible.

IV. Focused Laser Differential Interferometry (FLDI) Results

Boundary-layer instability measurements were performed during this testing campaign, and the results from these measurements supported the need to make efforts to clean the shock tube prior to experimentation. A benefit of working in T5 at this time is the extensive database of run conditions that have been established by prior researchers; the run condition database permits current researchers to perform experiments at specified Reynolds numbers and total enthalpy. For run conditions at lower Reynolds number, laminar response would be expected based on past heat-flux measurements. However, in some instances where laminar flow was expected, boundary-layer instability measurements revealed that a sporadic and unexplainable period of broadband response would pass through the probe volume of the focused laser differential interferometer (FLDI).^a

To show these occurrences, spectrograms of two runs are compared. An example of sporadic response shows a large swath of broad-band response, followed by a period where minimal disturbances are detected, followed by a period of narrowband response (Fig 3, (top)). This is in contrast to data recorded after the cleaning procedure was implemented, as in Fig. 3 (bottom). A stochastic but sensible series of narrowband peaks is observed. Hofferth et al.⁵ present spectrograms of slender-body hypersonic boundary-layer instability data obtained with the focused-schlieren method. This data, which appears as Fig. 7 in that work,⁵ was recorded in a low-disturbance facility, and appears qualitatively similar to the FLDI data in Fig. 3 (bottom).

During some experiments, the FLDI system would register near zero voltage just after the tunnel startup period (Fig. 4 left); this behavior inhibits FLDI measurement. Steady flow over the cone begins ≈ 1 ms after the trigger and lasts approximately 1 ms. The trigger is the primary shock wave registering a response by the reservoir pressure transducers, and indicates a reference time-zero for all data acquired in T5. Vibration is eliminated as a candidate cause of the FLDI blackout by accelerometer measurement. Small, constant amplitude vibrations begin at the test section ≈ 100 ms before the trigger. After $\approx 4 - 5$ ms from the trigger the vibration environment becomes harsh, but this is after the end of the test time, and does not affect the FLDI measurements. The vibration environment timing is approximately the same for all shots in T5. Details of these measurements can be found in Parziale.²⁰

We conclude that the difference in response between Fig. 4 (left) and (right) is that the gas is exhibiting characteristics consistent with opacity. The opacity may have been caused by material in the flow from an

^aThe FLDI^{18, 40-42} is an optical technique which permits the high-speed and non-intrusive interrogation of small-amplitude density perturbations.

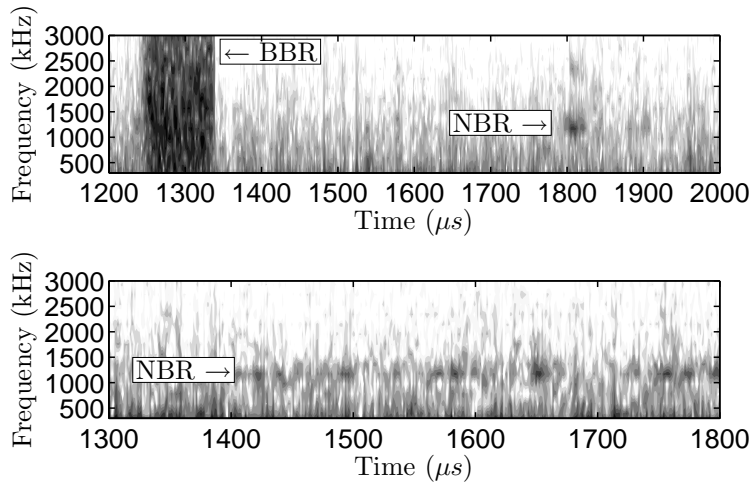


Figure 3. Arbitrary logarithmic units of change in density, the spectrum is estimated by the short time Fourier transform. Darker shading indicates larger amplitude. BBR is broadband response, NBR is narrowband response. *Top*: An example of sporadic response shows a large swath of broad-band response, followed by a period where minimal disturbances are detected, followed by a period of narrowband response (shot 2702). *Bottom*: An example of a stochastic but sensible series of narrowband peaks (shot 2789).

oxidation/ablation process in the shock tube or nozzle throat. The problem is more evident as the reservoir enthalpy is raised, and even more so as the reservoir pressure is raised. Consistently executing experiments near the T5 performance limits without the described cleaning procedures leads to results as in Fig. 4 (left). Following a rigorous cleaning procedure permits results as in Fig. 4 (right) to be reproducibly demonstrated.

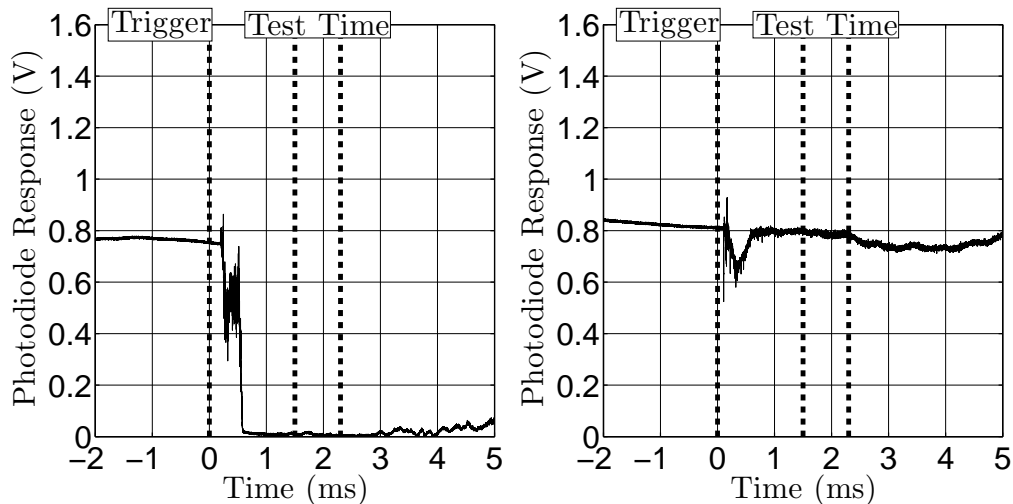


Figure 4. Raw time traces of photodiode response of the FLDI. The ordinate range represents the peak (0.0 volts) and trough (1.6 volts) of a fringe; before each experiment the interferometer set to the middle of a fringe, 0.8 volts. The dashed lines represent the data acquisition system **Trigger** and the **Test Time** period. *Left*: During startup period of shot 2726 (CO_2) the flow becomes opaque. *Right*: No opacity problems are evident for shot 2773 (N_2).

V. Transition Measurements

The main body of the cone was instrumented with a total of 80 flush-mounted thermocouples evenly spaced at 20 lengthwise locations beginning at 221 mm along the surface from the tip of the cone, with each row located 38 mm in the lengthwise direction from the last. These thermocouples have a response time on the order of a few microseconds and have been successfully used for boundary layer transition onset determination by Adam and Hornung,¹² Rasheed et al.,¹³ and Jewell et al.,²² as well as for tracking the propagation of turbulent spots by Jewell et al.¹⁷ Time- and spatially-resolved heat flux data allows the

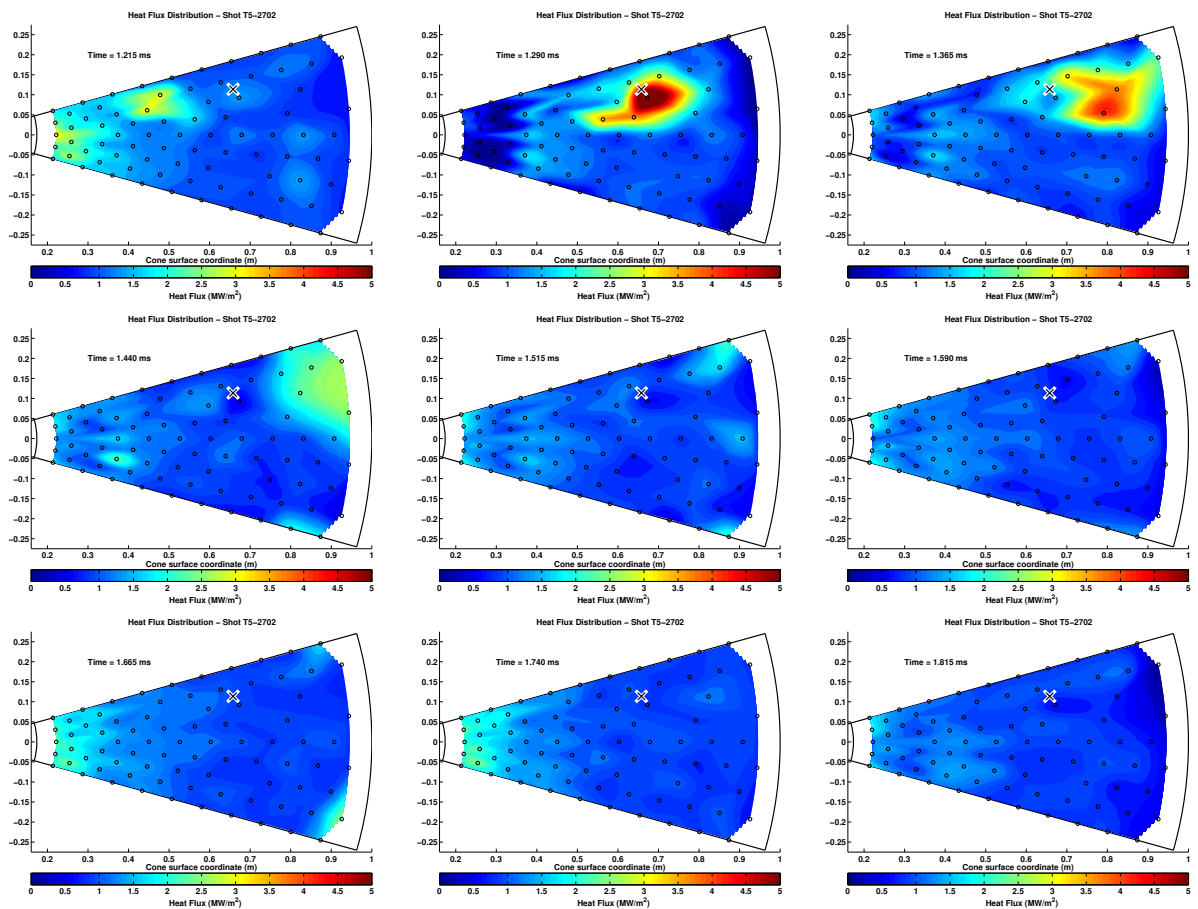


Figure 5. Heat flux frames from shot 2702 at 0.075 ms intervals covering a total time of 0.6 ms, during which a turbulent spot is observed (first frame, top left) and seen to propagate downstream and eventually off the end of the cone in the subsequent three frames. The location of the FLDI is marked with an “X” at 665 mm from the tip.

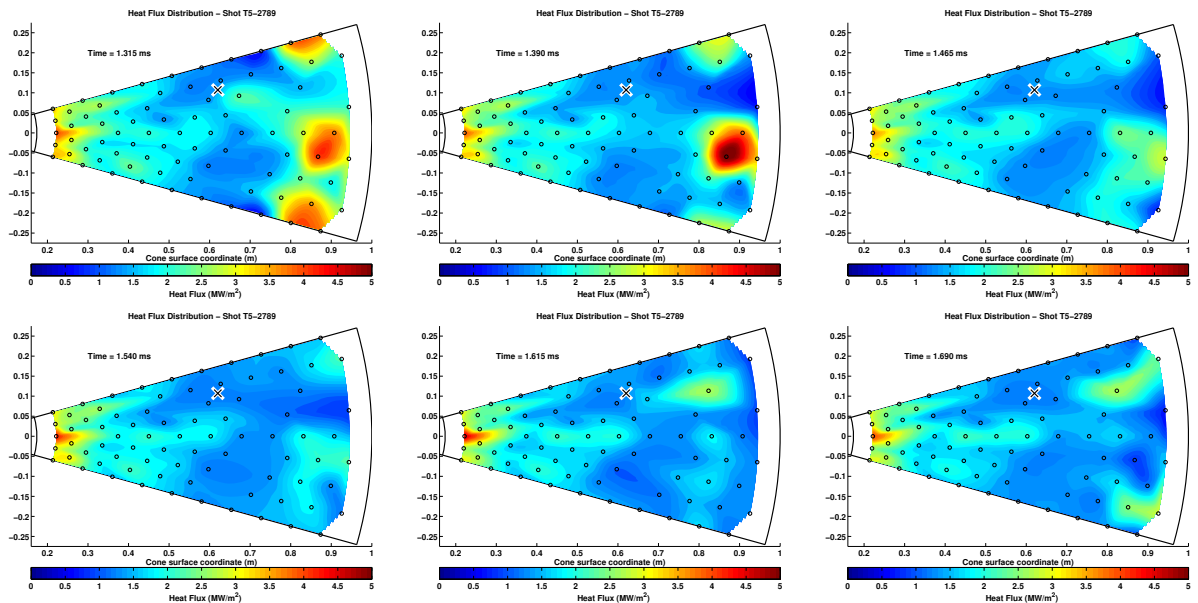


Figure 6. Heat flux frames from shot 2789 at 0.075 ms intervals covering a total time of 0.375 ms. While turbulent intermittency is observed near the end of the cone, no propagating turbulent bursts are visible during the experiment. The location of the FLDI is marked with an “X” at 627 mm from the tip.

presentation of a “movie” of heat flux over the entire instrumented surface of the cone by interpolating the processed thermocouple signals. Fig. 5 presents several heat flux frames from the test time of shot 2702 (corresponding to the FLDI result shown in the top half of Fig. 3), and Fig. 6 presents several heat flux frames from the test time of shot 2789 (corresponding to the FLDI result shown in the bottom half of Fig. 3). The boundary layer edge conditions for these two shots are recorded in Table 1. In the former result (2702), a turbulent spot is observed and seen to propagate downstream, crossing the location of the FLDI sensor at the same time as broadband response is observed in the spectrogram for shot 2702 (Fig. 3 (top) and Fig. 5 at $\approx 1250 - 1350 \mu\text{s}$). This spot is generated independently of the other transition events that are typically observed in natural transition and is therefore believed to be the result of particulate impact on the boundary layer during the test time. In the latter result (2789), no turbulent spots are observed near the FLDI during the test time, although turbulent intermittency typical of natural transition is observed near the end of the cone. This observation is consistent with the lack of broadband response observed in the spectrogram for shot 2789 (Fig. 3 (bottom) and Fig. 6).

Table 1. Summary of edge conditions for shots 2702 and 2789 in air.

Shot	h_{res} (MJ/kg)	P_{res} (MPa)	U_e (m/s)	P_e (kPa)	T_e (K)	T_{v_e} (K)	ρ_e (kg/m ³)	M_e (-)	unit Re_e (1/m)
2702	8.45	49.9	3680	36.9	1420	1419	0.090	4.84	6.61×10^6
2789	11.9	56.4	4250	47.1	2088	2088	0.077	4.57	4.78×10^6

VI. Transition Onset Correlations

In this section, we perform a statistical analysis of transition Reynolds number data. We seek correlations between transition Reynolds number and tunnel parameters for the purpose of assessing the ability to reproducibly prescribe transition locations via tunnel parameters. The ability to accurately and repeatedly prescribed transition location enables researchers to study the fundamentals of hypervelocity BLT. We chose the coefficient of determination of correlation between tunnel-parameters and transition Reynolds number as a metric. A higher coefficient of determination indicates higher repeatability, or fewer outliers.

Transition onset measurements, described in Jewell²³ and Jewell and Shepherd,⁴³ were more consistent in experiments after the shock tube cleaning procedures described in Section III were implemented ($n = 34$) than in those prior ($n = 40$). Jewell et al.^{23,44,45} showed that the tunnel parameters h_{res} and P_{res} could be used as predictor variables to construct statistically significant linear models for both the present data sets and the historical T5 transition data of Germain and Hornung¹¹ and Adam and Hornung¹² for air, CO₂, and N₂. In the present work, only air transition data is considered. These linear models take the form:

$$\text{Re}_{\text{Tr}}(P_{\text{res}}, h_{\text{res}}) = \text{Re}_{\text{intercept}} + C_{P_{\text{res}}} P_{\text{res}} + C_{h_{\text{res}}} h_{\text{res}}$$

Here, the coefficients that define the regression plane, $C_{P_{\text{res}}}$, $C_{h_{\text{res}}}$ and the Re intercept are computed using the MATLAB Statistics Toolbox. The regression plane fit to the clean tunnel results is presented along with the clean tunnel data in Fig. 7. The complete model results before the implementation of new shock tube cleaning procedures are recorded in Table 2, and the results after the implementation of the cleaning procedures are recorded in Table 3.

The position of the best-fit Re plane computed relative to the $h_{\text{res}}-P_{\text{res}}$ plane (*i.e.*, the intercept) is 5.90×10^5 for the dirty tunnel data and 1.83×10^6 for the clean tunnel data. The larger intercept value for the clean results is an indication that the tunnel cleaning procedure tends to increase transition onset Reynolds number. Moreover, the clean tunnel results are less scattered than the dirty results, which is consistent with the stochastic effect that would be expected in dirty flow from an unknown and probably inconsistent variation in particle size and number density, which Fedorov¹⁶ showed each have a significant influence on transition Reynolds number. Linear regression analysis performed using the tunnel parameters, reservoir enthalpy (h_{res}) and reservoir pressure (P_{res}), as the predictor variables and the edge Reynolds number at the transition onset location (Re_{Tr}) as the response variable had a modeled R^2 value of 0.50 for the experiments prior to cleaning procedure implementation, and an R^2 value of 0.80 subsequent to the implementation

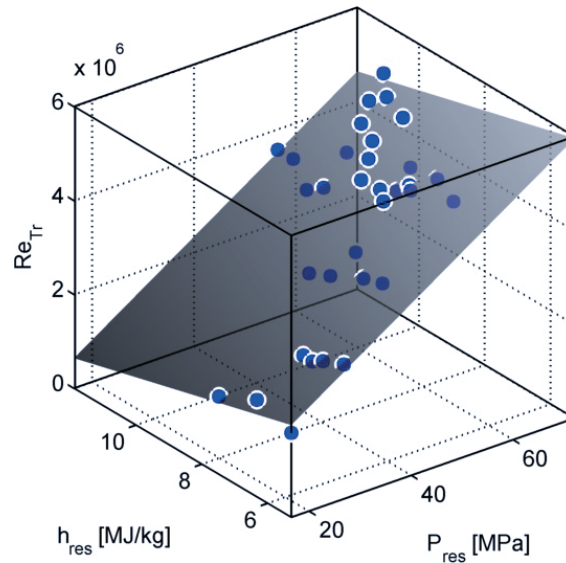


Figure 7. Regression plane ($R^2 = 0.80$) fit to “clean tunnel” Re_{Tr} data ($n = 34$) in reservoir enthalpy–reservoir pressure space. The Re (vertical) intercept of this plane is at $Re = 1.83 \times 10^6$ ($\pm 0.40 \times 10^6$).

of the cleaning procedure. When the same regression analysis is performed using the Reynolds number calculated at reference conditions at the transition onset location (Re_{Tr}^*), $R^2 = 0.70$ prior to cleaning procedure implementation and $R^2 = 0.86$ subsequently.

Table 2. Multivariable linear regression analyses with Re_{Tr} ($R^2 = 0.50$) and Re_{Tr}^* ($R^2 = 0.70$) as the response variables for “dirty” tunnel results ($n = 40$) acquired before the implementation of the new cleaning regimen. We use a significance level of 5% (*i.e.*, requiring a p -value less than 0.05 to reject the null hypothesis that a given coefficient is zero). The coefficients found to be statistically significant under this criterion are in bold print.

	Re_{Tr}	Re_{Tr}^*
Re intercept	5.90×10^5	-1.38×10^6
p -value	0.37394	0.00834
$C_{P_{res}}$	4.82×10^4	3.54×10^4
p -value	2.18×10^{-4}	2.99×10^{-4}
$C_{h_{res}}$	9.18×10^5	2.98×10^5
p -value	0.34578	2.12×10^{-4}

Table 3. Multivariable linear regression analyses with Re_{Tr} ($R^2 = 0.80$) and Re_{Tr}^* ($R^2 = 0.86$) as the response variables for “clean” tunnel results ($n = 34$) acquired after the implementation of the new cleaning regimen. The coefficients found to be statistically significant ($p < 0.05$) are in bold print.

	Re_{Tr}	Re_{Tr}^*
Re intercept	1.83×10^6	-1.08×10^5
p -value	6.86×10^{-5}	0.73991
$C_{P_{res}}$	7.20×10^4	3.54×10^4
p -value	2.30×10^{-10}	1.29×10^{-9}
$C_{h_{res}}$	-2.01×10^5	3.39×10^4
p -value	0.00718	0.55180

VII. Conclusions and Future Work

In this work, we emphasize the need for researchers utilizing impulse facilities for hypervelocity boundary-layer instability and transition research to operate the facility in a manner least likely to introduce particulate to the test flow. We compare FLDI (boundary-layer density disturbances) and heat transfer (surface mounted heat-transfer thermocouples) results before and after a cleaning regimen was implemented.

Prior to the implementation of the cleaning regimen, unpredictable turbulent spots were observed in both FLDI and thermocouple data at locations uncharacteristic of natural transition; we believe that it is likely these turbulent spots are the result of bypass transition initiated by particulate striking the model surface. Also prior to the implementation of the cleaning regimen, behavior consistent with flow opacity was observed in the FLDI data. Following the implementation of the cleaning regimen, these anomalous results have been nearly eliminated.

A statistical analysis which correlates tunnel parameters to transition location indicates that the coefficient of determination was significantly increased after the cleaning regimen implementation. We consider this increase in the coefficient of determination to be consistent with a more repeatable experiment. Most importantly, through careful selection of conditions and cleaning of the shock tube, it is possible to systematically prescribe transition locations on the test article in a repeatable manner. Jewell et al.^{22,23} estimate that the transition locations correspond to second-mode amplification factors e^N of $N \approx 8-12$. This ability to repeat transition locations facilitates hypervelocity boundary-layer stability and transition research.

Acknowledgments

The authors would like to thank Bahram Valiferdowski for help running T5 and Ross Wagnild for help with the program to compute the run conditions. This work was an activity that was part of National Center for Hypersonic Laminar-Turbulent Research, sponsored by the “Integrated Theoretical, Computational, and Experimental Studies for Transition Estimation and Control” project, supported by the U.S. Air Force Office of Scientific Research and the National Aeronautics and Space Administration (FA9552-09-1-0341). Additionally, this work was part of the “Transition Delay in Hypervelocity Boundary Layers by Means of CO₂/Acoustic Interactions” project, sponsored by the Air Force Office of Scientific Research (FA9550-10-1-0491). J. S. Jewell received additional support from the National Defense Science and Engineering Graduate Fellowship and the Jack Kent Cooke Foundation.

References

- ¹Bushnell, D., “Notes on Initial Disturbance Fields for the Transition Problem,” *Instability and Transition*, edited by M. Husaini and R. Voigt, ICASE/NASA LaRC Series, Springer US, 1990, pp. 217–232. doi: [10.1007/978-1-4612-3430-2_28](https://doi.org/10.1007/978-1-4612-3430-2_28).
- ²Schneider, S. P., “Effects of High-Speed Tunnel Noise on Laminar-Turbulent Transition,” *Journal of Spacecraft and Rockets*, Vol. 38, No. 3, 2001, pp. 323–333. doi: [10.2514/2.3705](https://doi.org/10.2514/2.3705).
- ³Schneider, S. P., “Hypersonic Laminar-Turbulent Transition on Circular Cones and Scramjet Forebodies,” *Progress in Aerospace Sciences*, Vol. 40, No. 1-2, 2004, pp. 1–50. doi: [10.1016/j.paerosci.2003.11.001](https://doi.org/10.1016/j.paerosci.2003.11.001).
- ⁴Schneider, S. P., “Development of Hypersonic Quiet Tunnels,” *Journal of Spacecraft and Rockets*, Vol. 45, No. 4, 2008, pp. 641–664. doi: [10.2514/1.34489](https://doi.org/10.2514/1.34489).
- ⁵Hofferth, J. W., Humble, R. A., Floryan, D. C., and Saric, W. S., “High-Bandwidth Optical Measurements of the Second-Mode Instability in a Mach 6 Quiet Tunnel,” *Proceedings of 51st AIAA Aerospace Sciences Meeting Including the New Horizons Forum and Aerospace Exposition*, AIAA 2013-0378, Grapevine, Texas, 2013. doi: [10.2514/6.2013-378](https://doi.org/10.2514/6.2013-378).
- ⁶Hofferth, J. W., Saric, W. S., Kuehl, J., Perez, E., and Reed, H., “Boundary-layer instability and transition on a flared cone in a Mach 6 quiet wind tunnel,” *International Journal of Engineering Systems Modelling and Simulation*, Vol. 5, No. 1-3, 2013, pp. 109–124. doi: [10.1504/IJESMS.2013.052386](https://doi.org/10.1504/IJESMS.2013.052386).
- ⁷Kocian, T. S., Perez, E., Oliviero, N. B., Kuehl, J. J., and Reed, H. L., “Hypersonic Stability Analysis of a Flared Cone,” *Proceedings of 51st AIAA Aerospace Sciences Meeting Including the New Horizons Forum and Aerospace Exposition*, AIAA 2013-0667, Grapevine, Texas, 2013. doi: [10.2514/6.2013-667](https://doi.org/10.2514/6.2013-667).
- ⁸Laurence, S. J., Wagner, A., Hannemann, K., Wartemann, V., Lüdeke, H., Tanno, H., and Itoh, K., “Time-Resolved Visualization of Instability Waves in a Hypersonic Boundary Layer,” *AIAA Journal*, Vol. 50, No. 6, 2012, pp. 243–246. doi: [10.2514/1.56987](https://doi.org/10.2514/1.56987).

- ⁹Laurence, S., Wagner, A., and Hannemann, K., "Schlieren-based techniques for investigating instability development and transition in a hypersonic boundary layer," *Experiments in Fluids*, Vol. 55, No. 8, 2014. doi: [10.1007/s00348-014-1782-9](https://doi.org/10.1007/s00348-014-1782-9).
- ¹⁰Laurence, S. J., Wagner, A., Ozawa, H., Schramm, J. M., and Hannemann, K., "Visualization of a hypersonic boundary-layer transition on a slender cone," *19th AIAA International Space Planes and Hypersonic Systems and Technologies Conference*, AIAA-2014-3110, Atlanta, Georgia, 2014.
- ¹¹Germain, P. D. and Hornung, H. G., "Transition on a Slender Cone in Hypervelocity Flow," *Experiments in Fluids*, Vol. 22, 1997, pp. 183–190. doi: [10.1007/s003480050036](https://doi.org/10.1007/s003480050036).
- ¹²Adam, P. H. and Hornung, H. G., "Enthalpy Effects on Hypervelocity Boundary-layer Transition: Ground Test and Flight Data," *Journal of Spacecraft And Rockets*, Vol. 34, No. 5, 1997, pp. 614–619. doi: [10.2514/2.3278](https://doi.org/10.2514/2.3278).
- ¹³Rasheed, A., Hornung, H. G., Fedorov, A. V., and Malmuth, N. D., "Experiments on Passive Hypervelocity Boundary-layer Control Using an Ultrasonically Absorptive Surface," *AIAA J.*, Vol. 40, No. 3, MAR 2002, pp. 481–489. doi: [10.2514/2.1671](https://doi.org/10.2514/2.1671).
- ¹⁴Jewell, J. S., Leyva, I. A., Parziale, N. J., and Shepherd, J. E., "Effect of Gas Injection on Transition in Hypervelocity Boundary Layers," *Proceedings of the 28th International Symposium on Shock Waves*, ISSW, Manchester, UK, 2011.
- ¹⁵Parziale, N. J., Jewell, J. S., Shepherd, J. E., and Hornung, H. G., "Optical Detection of Transitional Phenomena on Slender Bodies in Hypervelocity Flow," *Proceedings of AVT-200 Specialists' Meeting on Hypersonic Laminar-Turbulent Transition*, NATO, San Diego, California, 2012.
- ¹⁶Fedorov, A. V., "Receptivity of a supersonic boundary layer to solid particulates," *Journal of Fluid Mechanics*, Vol. 737, 2013, pp. 105–131. doi: [10.1017/jfm.2013.564](https://doi.org/10.1017/jfm.2013.564).
- ¹⁷Jewell, J. S., Parziale, N. J., Leyva, I. A., Shepherd, J. E., and Hornung, H. G., "Turbulent Spot Observations within a Hypervelocity Boundary Layer on a 5-degree Half-Angle Cone," *Proceedings of 42nd AIAA Fluid Dynamics Conference and Exhibit*, AIAA-2012-3062, New Orleans, Louisiana, 2012. doi: [10.2514/6.2012-3062](https://doi.org/10.2514/6.2012-3062).
- ¹⁸Parziale, N. J., Shepherd, J. E., and Hornung, H. G., "Differential Interferometric Measurement of Instability at Two Points in a Hypervelocity Boundary Layer," *Proceedings of 51st AIAA Aerospace Sciences Meeting Including the New Horizons Forum and Aerospace Exposition*, AIAA-2013-0521, Grapevine, Texas, 2013. doi: [10.2514/6.2013-521](https://doi.org/10.2514/6.2013-521).
- ¹⁹Parziale, N. J., Shepherd, J. E., and Hornung, H. G., "Differential Interferometric Measurement of Instability in a Hypervelocity Boundary Layer," *AIAA Journal*, Vol. 51, No. 3, 2013, pp. 750–754. doi: [10.2514/1.J052013](https://doi.org/10.2514/1.J052013).
- ²⁰Parziale, N. J., *Slender-Body Hypervelocity Boundary-Layer Instability*, Ph.D. thesis, [California Institute of Technology](https://www.proquest.com/docview/2131111111), 2013.
- ²¹Parziale, N. J., Shepherd, J. E., and Hornung, H. G., "Free-stream density perturbations in a reflected-shock tunnel," *Experiments in Fluids*, Vol. 55, No. 2, 2014, pp. 1–10. doi: [10.1007/s00348-014-1665-0](https://doi.org/10.1007/s00348-014-1665-0).
- ²²Jewell, J. S., Wagnild, R. M., Leyva, I. A., Candler, G. V., and Shepherd, J. E., "Transition Within a Hypervelocity Boundary Layer on a 5-Degree Half-Angle Cone in Air/CO₂ Mixtures," *51st AIAA Aerospace Sciences Meeting including the New Horizons Forum and Aerospace Exposition*, AIAA-2013-0523, Grapevine, Texas, 2013. doi: [10.2514/6.2013-523](https://doi.org/10.2514/6.2013-523).
- ²³Jewell, J. S., *Boundary-Layer Transition on a Slender Cone in Hypervelocity Flow with Real Gas Effects*, Ph.D. thesis, [California Institute of Technology](https://www.proquest.com/docview/2131111111), Pasadena, CA, 2014.
- ²⁴Gronvall, J. E., Johnson, H. B., and Candler, G. V., "Boundary-Layer Stability Analysis of High Enthalpy Shock Tunnel Transition Experiments," *Journal of Spacecraft and Rockets*, Vol. 51, 2014, pp. 455–467. doi: [10.2514/1.A32577](https://doi.org/10.2514/1.A32577).
- ²⁵Tanno, H., Komura, T., Sato, K., Itoh, K., Takahashi, M., and Fujii, K., "Measurements of Hypersonic Boundary Layer Transition on Cone Models in the Free-Piston Shock Tunnel HIEST," *Proceedings of 47th AIAA Aerospace Sciences Meeting including The New Horizons Forum and Aerospace Exposition*, AIAA, Orlando, FL, 2009.
- ²⁶Hornung, H. G., "Performance Data of the New Free-Piston Shock Tunnel at GALCIT," *Proceedings of 17th AIAA Aerospace Ground Testing Conference*, AIAA 1992-3943, Nashville, TN, 1992. doi: [10.2514/6.1992-3943](https://doi.org/10.2514/6.1992-3943).
- ²⁷Goodwin, D. G., "An Open-Source, Extensible Software Suite for CVD Process Simulation," *Proceedings of CVD XVI and EuroCVD Fourteen, M Allendorf, F Maury, and F Teyssandier (Eds.)*, 2003, pp. 155–162.
- ²⁸Browne, S., Ziegler, J., and Shepherd, J. E., "Numerical Solution Methods for Shock and Detonation Jump Conditions," GALCIT - FM2006-006, 2006.
- ²⁹Gordon, S. and McBride, B., "Thermodynamic Data to 20000 K for Monatomic Gases," NASA TP-1999-208523, 1999.
- ³⁰McBride, B. J., Zehe, M. J., and Gordon, S., "NASA Glenn Coefficients for Calculating Thermodynamic Properties of Individual Species," NASA TP-2002-211556, 2002.
- ³¹Candler, G. V., "Hypersonic Nozzle Analysis Using an Excluded Volume Equation of State," *Proceedings of 38th AIAA Thermophysics Conference*, AIAA-2005-5202, Toronto, Ontario Canada, 2005. doi: [10.2514/6.2005-5202](https://doi.org/10.2514/6.2005-5202).
- ³²Wagnild, R. M., *High Enthalpy Effects on Two Boundary Layer Disturbances in Supersonic and Hypersonic Flow*, Ph.D. thesis, University of Minnesota, Minnesota, 2012.
- ³³Spalart, P. R. and Allmaras, S. R., "A One-equation Turbulence Model for Aerodynamic Flows," *Proceedings of 30th AIAA Aerospace Sciences Meeting and Exhibit*, AIAA 1992-439, Reno, Nevada, 1992. doi: [10.2514/6.1992-439](https://doi.org/10.2514/6.1992-439).
- ³⁴Catrisa, S. and Aupoix, B., "Density Corrections for Turbulence Models," *Aerospace Science and Technology*, Vol. 4, No. 1, 2000, pp. 1–11. doi: [10.1016/S1270-9638\(00\)00112-7](https://doi.org/10.1016/S1270-9638(00)00112-7).
- ³⁵Johnson, H. B., *Thermochemical Interactions in Hypersonic Boundary Layer Stability*, Ph.D. thesis, University of Minnesota, Minnesota, 2000.
- ³⁶Johnson, H. B., Seipp, T. G., and Candler, G. V., "Numerical Study of Hypersonic Reacting Boundary Layer Transition on Cones," *Physics of Fluids*, Vol. 10, No. 13, 1998, pp. 2676–2685. doi: [10.1063/1.869781](https://doi.org/10.1063/1.869781).

- ³⁷Taylor, J. R. and Hornung, H. G., "Real gas and wall roughness effects on the bifurcation of the shock reflected from the end wall of a tube," *Proceedings of the 13th International Symposium on Shock Waves*, ISSW, Niagara Falls, NY USA, 1981.
- ³⁸Mark, H., "The Interaction of a Reflected Shock Wave with the Boundary Layer in a Shock Tube," NACA TM-1418, 1958.
- ³⁹Davies, L. and Wilson, J. L., "Influence of Reflected Shock and Boundary-Layer Interaction on Shock-Tube Flows," *Physics of Fluids*, Vol. 12, No. 5, 1969, pp. 137. doi: [10.1063/1.1692625](https://doi.org/10.1063/1.1692625).
- ⁴⁰Smeets, G., "Laser Interferometer for High Sensitivity Measurements on Transient Phase Objects," *IEEE Transactions on Aerospace and Electronic Systems*, Vol. AES-8, No. 2, 1972, pp. 186–190. doi: [10.1109/TAES.1972.309488](https://doi.org/10.1109/TAES.1972.309488).
- ⁴¹Smeets, G., "Laser-Interferometer mit grossen, fokussierten Lichtbündeln für lokale Messungen," ISL - N 11/73, 1973.
- ⁴²Smeets, G., "Verwendung eines Laser-Differentialinterferometers zur Bestimmung lokaler Schwankungsgrössen sowie des mittleren Dichteprofiles in einem turbulenten Freistrahle," ISL - N 20/74, 1974.
- ⁴³Jewell, J. S. and Shepherd, J. E., "T5 Conditions Report: Shots 2526–2823," Tech. rep., California Institute of Technology, Pasadena, CA, June 2014, [GALCIT Report FM2014.002](https://arc.aiaa.org).
- ⁴⁴Jewell, J. S., Shepherd, J. S., and Leyva, I. A., "Shock tunnel operation and correlation of boundary layer transition on a cone in hypervelocity flow," *Proceedings of the 29th International Symposium on Shock Waves*, ISSW29-000300, Madison, WI, July 2013.
- ⁴⁵Jewell, J. S., Shepherd, J. S., and Leyva, I. A., "Supplemental data for 'Shock tunnel operation and correlation of boundary layer transition on a cone in hypervelocity flow'," Available at: <http://www.joejewell.com>, California Institute of Technology, July 2013.